Biochimica et Biophysica Acta, 691 (1982) 309–320
Elsevier Biomedical Press

BBA 71354

CHARACTERIZATION OF THE SUB-TRANSITION OF HYDRATED DIPALMITOYLPHOSPHATIDYLCHOLINE BILAYERS

KINETIC, HYDRATION AND STRUCTURAL STUDY

MARTIN J. RUOCCO and G. GRAHAM SHIPLEY

Biophysics Institute, Departments of Medicine and Biochemistry, Boston University School of Medicine, 80 East Concord Street, Boston, MA 02118 (U.S.A.)

(Received May 5th, 1982)

Key words: Phosphatidylcholine bilayer; Differential scanning calorimetry; X-ray diffraction; Sub-transition; Chain packing

Differential scanning calorimetry and fast-recording X-ray diffraction methods are used to study the kinetics, hydration and structural changes of the $L_{\beta'}$ gel → L_c 'crystal' conversion at −2°C for less than maximally hydrated (27.2 wt% H_2O) and maximally hydrated (48.9 wt% H_2O) 1,2-dipalmitoyl-L-phosphatidylcholine (DPPC) dispersions. Equilibration of DPPC dispersions at −2°C for increasing time periods results in a progressive increase in the sub-transition temperature to a limiting value of 17–19°C, while the enthalpy of the sub-transition also increases on reaching an enthalpy maximum $\Delta H = 5.6$–5.8 kcal/mol DPPC after 2 days equilibration. Corresponding X-ray diffraction experiments demonstrate two time domains involving structural alterations. An initial time domain involves a rapid shift of the two characteristic $L_{\beta'}$ wide angle reflections, 1/4.18 $Å^{-1}$ and 1/4.08 $Å^{-1}$, to 1/4.3 $Å^{-1}$ and 1/4.0 $Å^{-1}$, respectively, while there is no significant change in the lamellar periodicity. A slower structural alteration subsequently occurs involving a progressive decrease in lamellar periodicity to its limiting dimension, $d \cong 59.5$ Å and further shifts in the two wide angle reflections to final values of 1/4.4 $Å^{-1}$ and 1/3.86 $Å^{-1}$. These changes are indicative of alterations in both the bilayer organization and the hydrocarbon chain packing. Hydration studies over the range 10.1 to 48.9 wt% H_2O demonstrate that at 4°C the L_c bilayer phase has a reduced hydration limit of 11 mol H_2O/mol DPPC compared to 19 mol H_2O/mol DPPC and 25 mol H_2O/mol DPPC for the $L_{\beta'}$ and L_α bilayer phases, respectively. It is concluded that the $L_{\beta'} \rightarrow L_c$ conversion involves dehydration and hydrocarbon chain ordering. The data suggest a crystallization of DPPC and 11 H_2O molecules presumably involving tightly bound water molecules in an interbilayer matrix characterized by water-water and water-DPPC hydrogen bonding. A structural interpretation of the changes occurring in the two-dimensional hydrocarbon chain packing modes during the transitions between the hydrated L_c, $L_{\beta'}$, $P_{\beta'}$ and L_α bilayer forms of DPPC is proposed.

Introduction

The structure and physical properties of hydrated 1,2-diacyl-L-phosphatidylcholines (PC) have been studied in great detail. For example, a combination of calorimetric and X-ray diffraction studies identified and characterized two transitions corresponding to lamellar gel → gel ($L_{\beta'} \rightarrow P_{\beta'}$) and gel → liquid crystal ($P_{\beta'} \rightarrow L_\alpha$) bilayer interconversions for a series of PC in which the chain length is varied [1–6]. For hydrated 1,2-dipalmitoyl-L-phosphatidylcholine (DPPC) these reversible transitions occur at approx. 35 and 41°C, respectively. Chen et al. [7] recently showed, using high precision scanning calorimetry, that the DPPC-water $L_{\beta'}$ gel phase converts to a different low tempera-

ture form when held at 0°C for prolonged periods of time. This low temperature form exhibits a third low temperature sub-transition at ~ 18°C. Utilizing a similar experimental approach Füldner [8] and we [9] showed independently by X-ray diffraction that the low temperature form has a highly ordered structure with a more ordered hydrocarbon chain packing arrangement than the $L_{\beta'}$ gel phase. Furthermore, it was shown that the sub-transition corresponds to a structural transformation from the ordered low temperature 'crystalline' L_c form to the conventional $L_{\beta'}$ bilayer gel [8,9].

In this paper we describe the kinetic aspects of the formation of the low temperature 'crystal' form utilizing differential scanning calorimetry and fast-recording X-ray diffraction methods. In addition we compare the hydration characteristics of the low temperature 'crystal' phase with the hydration of the previously studied $L_{\beta'}$ gel and L_α liquid crystal bilayer phases [6].

Materials and Methods

Commercial grade DPPC (Sigma, St. Louis, MO) was shown to be >99% pure by thin-layer chromatography using chloroform/methanol/water/acetic acid (65:25:4:1, v/v) as eluting solvent. Hydrated DPPC multilamellar dispersions were prepared by centrifuging weighed amounts of DPPC and water through a narrow constriction in a sealed glass tube at 50°C. Different weight ratios of DPPC and water were utilized. DPPC dispersions were then transferred to stainless steel calorimetry pans and/or X-ray diffraction capillary tubes and stored at −4°C for different periods of time.

For DSC studies, the calorimetry pans were transferred at low temperature (0°C) to the scanning calorimeter pre-equilibrated at −2°C prior to transfer of samples. Following an initial DSC heating run, samples were then rapidly cooled to −2°C and held at that temperature for different periods of time, after which another heating run was performed. This process was repeated for increasing equilibration time periods, up to 66 h, at −2°C. To investigate longer term equilibration (up to 13 days), samples were removed from the calorimeter and stored in a freezer at −4°C. Following long term equilibration, samples were transferred to the calorimeter at 0°C, as described above.

For X-ray diffraction studies, the sample capillary tubes were again transferred at low temperature (0°C) to the X-ray diffraction sample holder pre-equilibrated at −2°C prior to transfer. Following recording of an X-ray diffraction pattern at −2°C, the sample was then heated to 20°C, the X-ray diffraction pattern recorded, and then rapidly cooled to −2°C. X-ray diffraction patterns were recorded continuously as a function of storage time at −2°C. In some cases the initial sample transfer was performed at 20°C, a diffraction pattern recorded at 20°C, and then rapidly cooled to 2°C, followed by the protocol described above.

Differential scanning calorimetry (DSC) over the heating range −10 to 50°C was performed using a Perkin-Elmer (Norwalk, CT) DSC-2 instrument. Each sample was heated and cooled at a rate of either 2.5 or 5.0 K/min. Transition temperatures were determined as the onset of the endothermic or exothermic transition extrapolated to the baseline. The weight of DPPC in the pan was determined gravimetrically and by phosphorus determination [10] of the pan contents. Good agreement between the two methods was observed. Enthalpy measurements were determined from the area under the transition peak by comparison with those for a known standard, gallium.

X-ray diffraction data were recorded using a position-sensitive detector counter method as described previously [9]. Nickel filtered CuK_α X-radiation ($\lambda = 1.5418$ Å) from a microfocus X-ray generator (Jarrel-Ash, Waltham, MA) was line focussed by a single mirror and collimated using the slit optical system of a Luzzati-Baro camera. X-ray diffraction data were recorded using a linear position sensitive detector (Tennelec, Oak Ridge, TN) and associated electronics (Tracor Northern, Middleton, WI). In all cases samples were contained in thin walled capillary tubes (internal diameter 1.0 mm) and mounted in variable temperature sample holders. Temperature stability was ±1 K.

Results

For studies of the kinetics of the appearance of the sub-transition, DSC and X-ray diffraction ex-

periments were performed on DPPC samples containing 27.2 wt% water and 48.9 wt% water. The former sample represents a hydration level corresponding to less than maximal hydration in the $L_{\beta'}$, $P_{\beta'}$ and L_{α} phases; the latter sample provides data corresponding to maximally hydrated phases. Results from these two systems will be described separately.

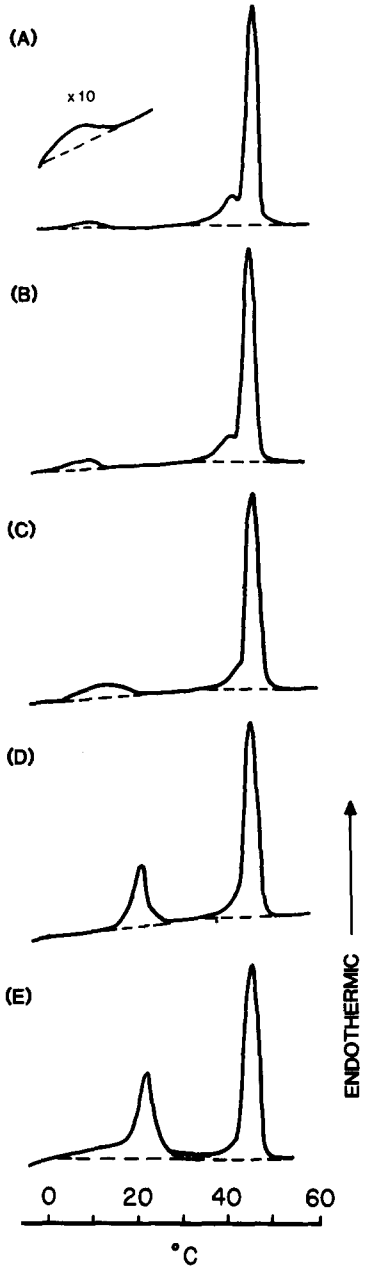

Fig. 1. Initial DSC heating curves of DPPC/27.2 wt% H_2O dispersions following rapid cooling from 20°C and subsequent equilibration at −2°C for different periods of time. (A) Immediate heating run from −2°C after rapid cooling from 20°C; (B) after 40 min equilibration at −2°C; (C) after 5 h equilibration at −2°C; (D) after 15 h equilibration at −2°C; (E) after 66 h equilibration at −2°C. Heating rate, 5 K/min.

DPPC/water (27.2 wt%)

DSC heating curves of hydrated DPPC following rapid cooling from 20°C and equilibration at −2°C for increasing periods of time (up to 66 h) are shown in Fig. 1. Immediate reheating shows a small but detectable sub-transition endotherm centered at approx. 7°C with transition onset $T_c = -1.6$°C. Characteristic endotherms corresponding to the pre- and main transitions occur at $T_c = 36.0$ and 41.8°C, respectively (Fig. 1A). After 40 min equilibration at −2°C, the low temperature transition increases in both temperature ($T_c = 0.8$°C) and enthalpy (Fig. 1B). Further storage for 5, 15 and 66 h results in a progressive increase in the transition temperature (limiting $T_c = 17.3$°C) and enthalpy of the sub-transition (Figs. 1C, D and E). At this low hydration level, with progressive storage at −2°C, the enthalpy associated with the pre-transition at $T_c = 37$°C diminishes such that after 15 h storage no obvious pre-transition is observed.

The enthalpy associated with the sub-transition is plotted as a function of equilibration time at −2°C in Fig. 2. The transition enthalpy shows a progressive increase with storage time and after

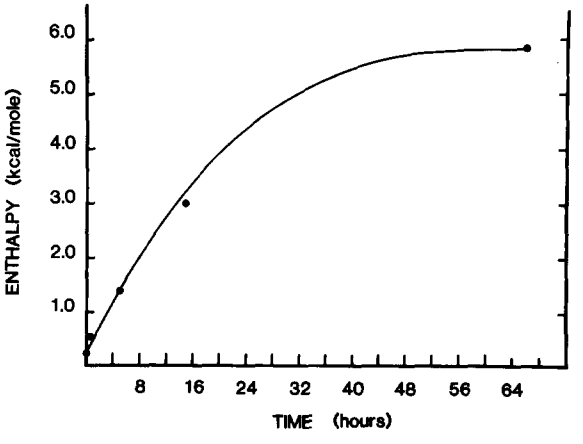

Fig. 2. Plot of sub-transition, ΔH (kcal/mol DPPC) of DPPC/27.2 wt% H_2O dispersions as a function of equilibration time at −2°C.

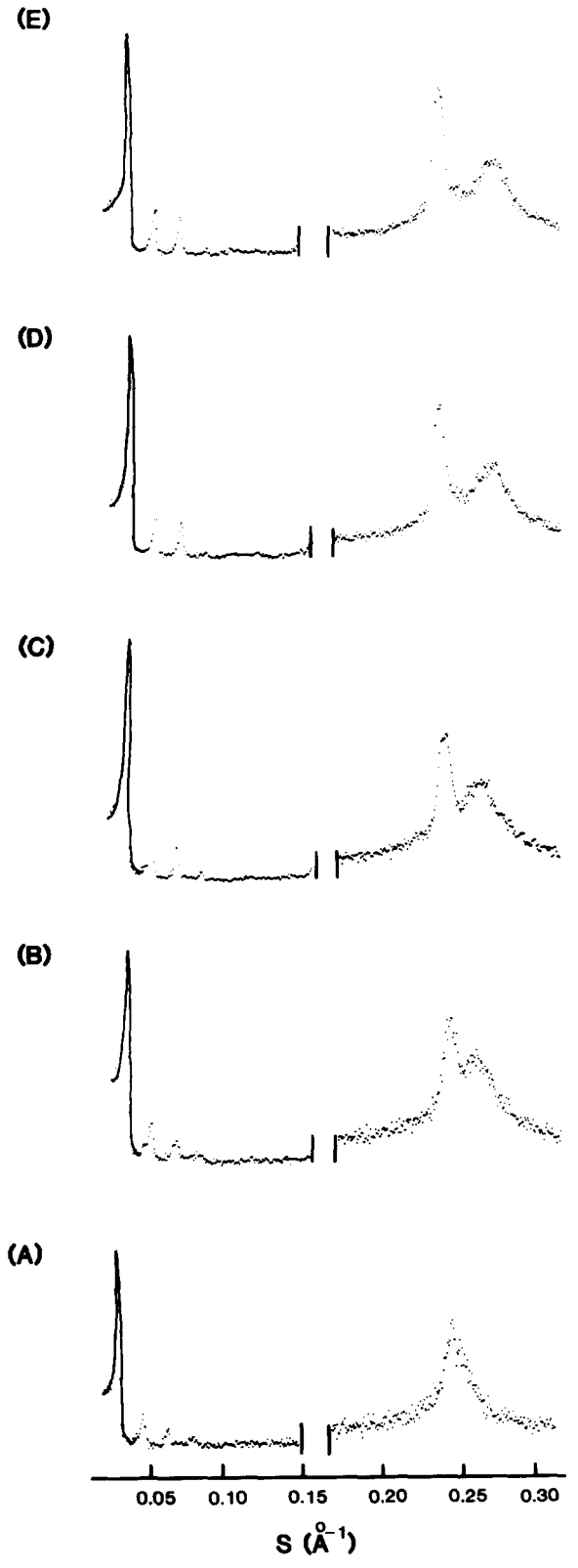

66 h reaches a value of 5.8 kcal/mol DPPC. This enthalpy value is significantly higher than that recorded previously for the sub-transition of maximally hydrated DPPC [7–9]. Similar high enthalpies associated with the sub-transition of DPPC following long term equilibration have recently been reported by Magni and Sheridan [11].

Fig. 3A shows the X-ray diffraction pattern for this sample, equilibrated and recorded at 20°C. The diffraction pattern shows lamellar spacings of periodicity 62.5 Å and a strong 1/4.18 $Å^{-1}$ wide-angle reflection with a shoulder at 1/4.09 $Å^{-1}$. This is characteristic of the lamellar $L_{\beta'}$ bilayer gel phase described earlier [2,4–6,8,9]. The sample was then cooled rapidly to −2°C. At −2°C successive 5-min accumulations were recorded up to 40 min and the summation of the diffraction patterns over this first 40 min period is shown in Fig. 3B. There is no significant change in the bilayer periodicity (62.4 Å); however, the wide-angle region already shows clear evidence of two quite well separated reflections at 1/4.29 and 1/4.00 $Å^{-1}$. Continued accumulations were made up to 70 h. The diffraction pattern accumulated over the time period 3–4 h is shown in Fig. 3C. Only a small decrease in bilayer period to 61.8 Å is evident. The wide-angle region shows more pronounced separation of the two wide-angle reflections to 1/4.32 and 1/3.98 $Å^{-1}$. Significant reductions in the bilayer periodicity are observed after 12 and 20 h (60.1 and 59.5 Å, respectively) and progressive, albeit small, changes in the intensity distribution of the lamellar reflections are apparent (Figs. 3D and 3E). The two strong wide-angle reflections reach limiting values of 1/4.40 and 1/3.86 $Å^{-1}$.

Changes in the bilayer periodicity and the positions of the two prominent wide-angle reflections are shown in Fig. 4. There appear to be two time domains over which distinctive structural changes

Fig. 3. X-ray diffraction patterns of DPPC/27.2 wt% H_2O dispersions. (A) 20°C in the $L_{\beta'}$ form. Following cooling from 20°C to −2°C, diffraction patterns were recorded: 0–40 min (B); 3–4 h (C); 11–12 h (D); 19–20 h (E). The diffraction data were recorded using a line-focussed X-ray beam and linear position sensitive detector. The sample to detector distance was 124.7 mm. Relative intensity is plotted on the ordinate and $s = 2\sin\theta/\lambda$ on the abscissa (2θ is the diffraction angle and λ the X-ray wavelength.

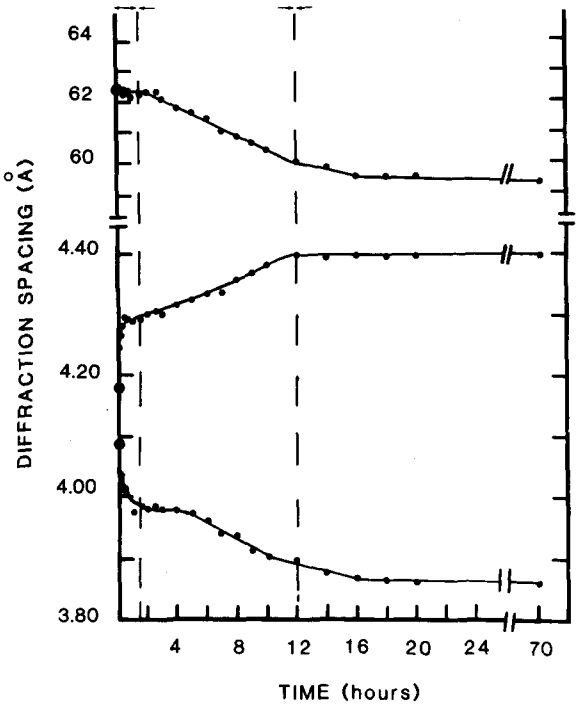

Fig. 4. Plot of the bilayer periodicity and positions of the two major wide-angle reflections of DPPC/27.2 wt% H_2O dispersions as a function of equilibration time at −2°C.

occur. In the wide angle region, the initial time points (within the first 10 min) at −2°C show diffraction patterns similar to that of the $L_{\beta'}$ form recorded at 20°C (large circles, Fig. 4). Up to approximately 1.5 h (dashed line, Fig. 4) large changes in the position and separation of the two major wide-angle reflections occur (see Fig. 3B, for example). However, during this time period the bilayer periodicity (lipid bilayer + intercalated water thickness) shows no significant change (d = 62.3 Å). In the time period approx. 2 to 12 h, a progressive decrease in bilayer periodicity from 62.3 to 59.5 Å is observed. This is accompanied by further separation of the two wide-angle reflections to limiting values of 1/4.40 and 1/3.86 $Å^{-1}$.

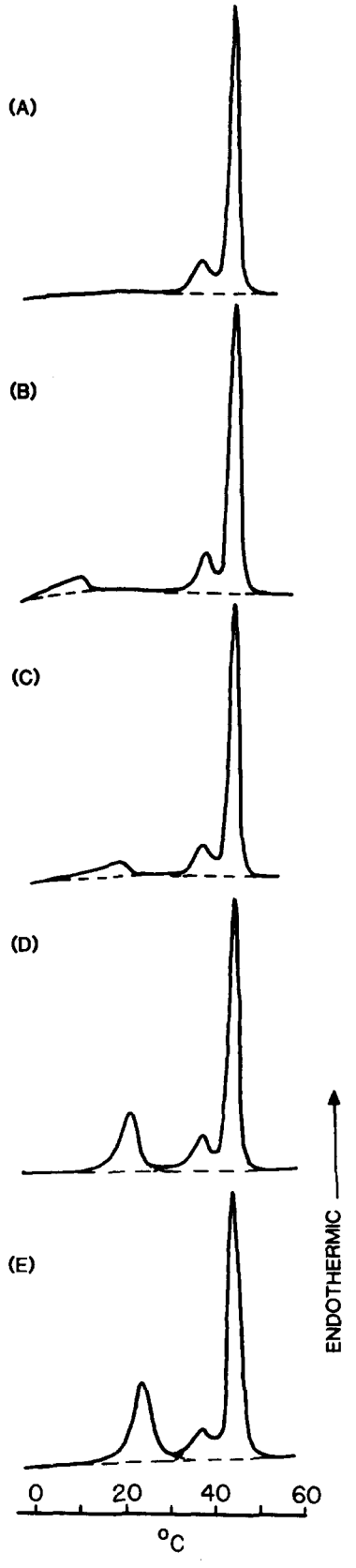

Fig. 5. Initial DSC heating curves of DPPC/48.9 wt% H_2O dispersions following rapid cooling from 20°C and subsequent equilibration at −2°C for different periods of time. (A) Immediate heating from −2°C after rapid cooling from 20°C; (B) after 40 min equilibration at −2°C; (C) after 4 h equilibration at −2°C; (D) after 14 h equilibration at −2°C; (E) after 66 h equilibration at −2°C. Heating rate, 5 K/min.

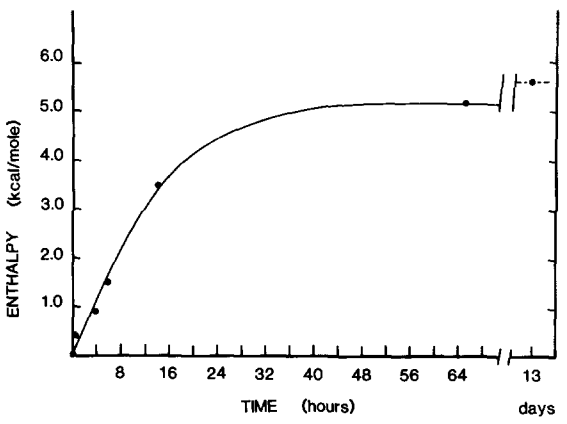

Fig. 6. Plot of sub-transition enthalpy, ΔH (kcal/mol DPPC) of DPPC/48.9 wt% H_2O dispersions as a function of equilibration time at $-2°C$.

After approx. 12 h, there appear to be no significant changes in either the bilayer periodicity (59.5 Å) or wide-angle reflections (1/4.40 and 1/3.86 $Å^{-1}$), at least up to 70 h incubation at $-2°C$.

DPPC/water (48.9 wt%)

Overall, a similar pattern of behavior is observed at this higher water content (Figs. 5–8). Fig. 5 shows DSC data of fully hydrated DPPC held at $-2°C$ for increasing periods of time. Immediate reheating shows no evidence of the sub-transition, but the characteristic pre- and main transitions occur at 32.8 and 41.3°C, respectively (Fig. 5A). Equilibration up to 66 h results in the appearance of the sub-transition. A progressive increase in sub-transition temperature and enthalpy with incubation time at $-2°C$ is observed (Figs. 5B–5E). No significant changes in either the transition temperature or enthalpies of the pre- and main transitions are observed as a function of incubation time. At 66 h the following values are obtained: sub-transition, onset temperature = 18.6°C, peak temperature = 22.8°C, $\Delta H = 5.2$ kcal/mol DPPC; (2) pre-transition, onset temperature = 32.3°C, peak temperature = 36.8°C, ΔH

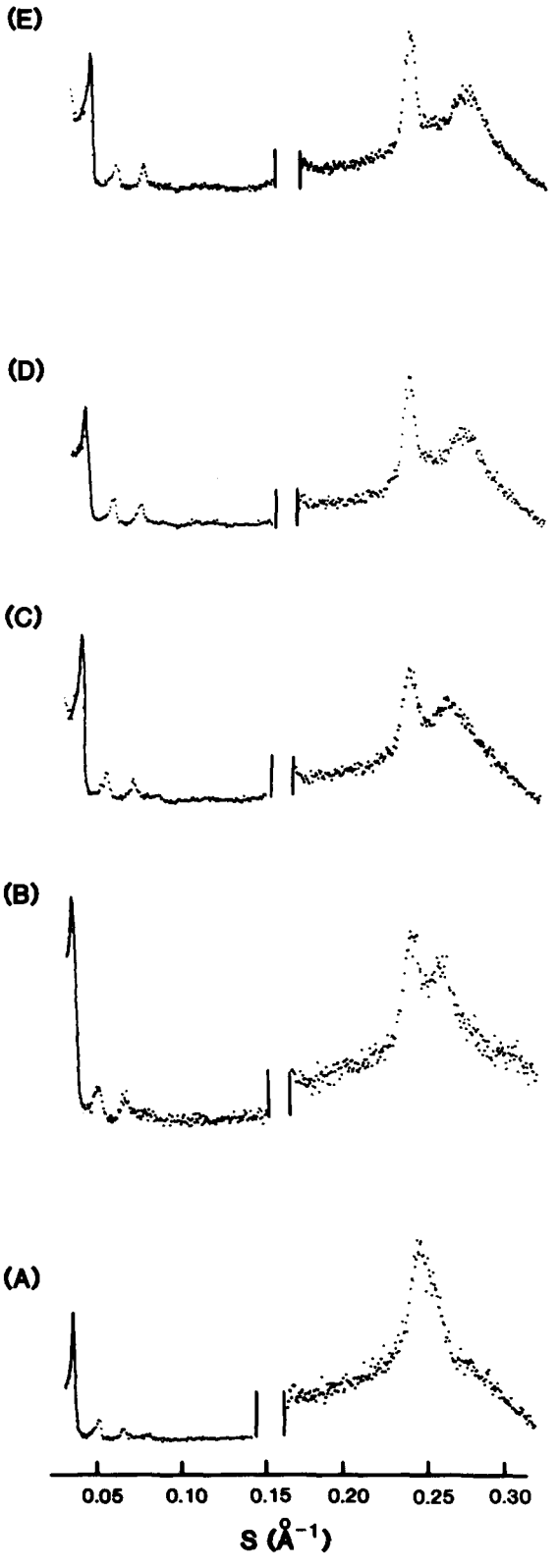

Fig. 7. X-ray diffraction patterns of DPPC/48.9 wt% H_2O dispersions. (A) 20°C in the $L_{\beta'}$ form. Following cooling from 20°C to $-2°C$, diffraction patterns were recorded: 0–40 min (B); 4.3–5.3 h (C); 10.3–11.3 h (D); 18.3–19.3 h (E). Sample to detector distance, 125.3 mm.

= 1.8 kcal/mol DPPC; (3) main transition, onset temperature = 41.8°C, peak temperature = 43.6°C, ΔH = 9.0 kcal/mol DPPC.

A progressive increase in the enthalpy of the sub-transition is observed, reaching a value of ΔH = 5.6 kcal/mol DPPC at 13 days (Fig. 6). This pattern of behavior is similar to that observed at lower hydration (cf. Figs. 2 and 6).

Corresponding X-ray diffraction experiments are summarized in Figs. 7 and 8. Fig. 7A shows a characteristic diffraction pattern of fully hydrated DPPC at 20°C in the $L_{\beta'}$ bilayer phase (bilayer periodicity = 63.5 Å; wide-angle reflections 1/4.18 $Å^{-1}$, 1/4.08 $Å^{-1}$ (shoulder). As illustrated in Figs. 7B–7E, the two wide-angle reflections progressively separate, reaching limiting values of 1/4.40 and 1/3.87 $Å^{-1}$ (see Fig. 7E, data accumulated at 19.3 h).

Again, changes in the structural parameters as a function of incubation time at −2°C show three apparent time domains (Fig. 8): (1) 0–1.5 h, significant changes in the positions of the two major wide-angle reflections with no significant change in bilayer periodicity; (2) 1.5–12 h, a decrease in bilayer periodicity accompanied by further changes in the positions of the wide angle reflections; (3) > 12 h, no further changes in either bilayer periodicity (59.4 Å) or wide-angle reflections (1/4.40 $Å^{-1}$ and 1/3.87 $Å^{-1}$).

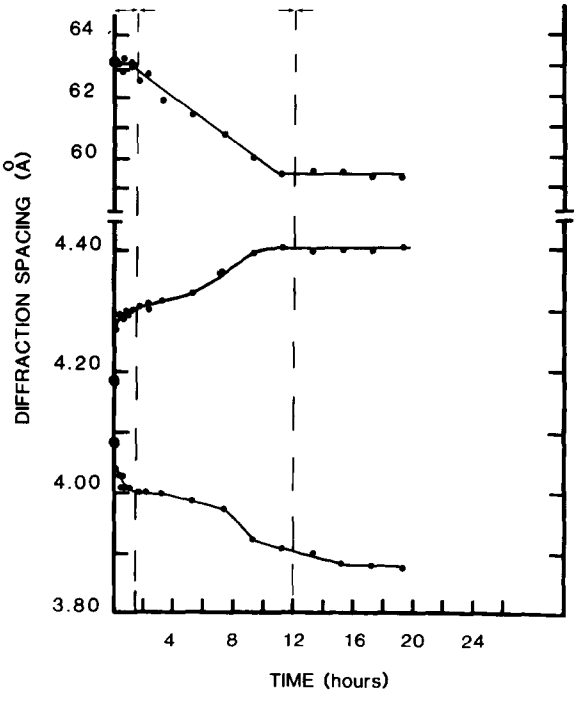

Fig. 8. Plot of the bilayer periodicity and positions of the two major wide-angle reflections of DPPC/48.9 wt% H_2O dispersions as a function of equilibration time at −2°C.

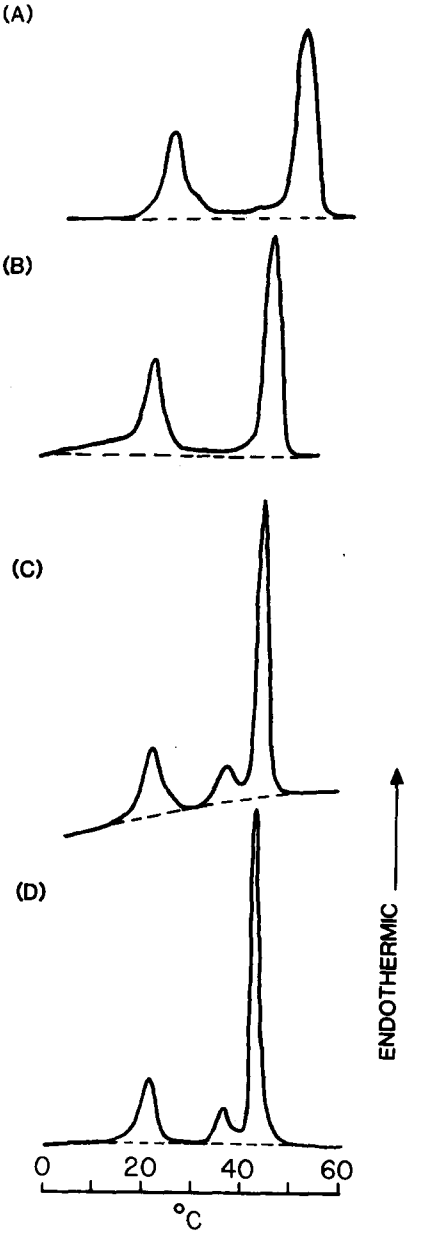

Fig. 9. Representative initial DSC heating curves of hydrated DPPC following prolonged storage at −4°C. (A) DPPC/13.9 wt% H_2O; (B) DPPC/27.2 wt% H_2O; (C) DPPC/48.9 wt% H_2O; (D) DPPC/93.9 wt% H_2O. Heating rate, 5 K/min.

DPPC hydration study

DPPC samples were equilibrated with various amounts of water (10.1–48.9 wt% water) using the constricted tube method and samples taken for DSC and X-ray diffraction. Following storage at −4°C for prolonged periods (>3 days) samples were transferred at low temperature and initial DSC heating curves recorded between 0 and 60°C. Representative DSC heating curves are shown in Figs. 9A–9C. At 13.9 wt% water only the sub- and main transitions (21.3 and 47.6°C, respectively) were observed. At 27.2 wt% water again only the sub-transition and main transition were observed (17.3 and 42.0°C). Although no pre-transition is observed on the initial heating run following prolonged storage at −4°C, subsequent cooling and heating runs do show evidence of this pre-transition (see, for example Fig. 1A). At 48.9 wt% water, the initial heating run clearly shows all three sub-, pre- and main transitions at the expected temperatures (see above). For comparison, the initial heating curve of DPPC in a large aqueous excess (93.9 wt% water) is shown in Fig. 9D. Identical calorimetric behavior is observed compared to that at 48.9 wt% water.

Since sub-transitions are observed for DPPC at all hydration levels between 10.1 and 93.9 wt% water, X-ray diffraction studies of the low temperature phase as a function of water content were performed. Diffraction patterns of the phase present below the sub-transition were recorded at 4°C. This phase exhibits an increase in bilayer periodicity from 55.0 to 59.3 Å over the hydration range 10.1 to 20 wt% water (Fig. 10A). No further increase in bilayer periodicity occurs from 20 to 48.9 wt% water. Thus the hydration limit for this phase is 20 wt% water.

Similar X-ray diffraction data were recorded at 20 and 60°C, temperatures at which at equilibrium only the $L_{\beta'}$ and L_α phases, respectively, are present. At 20°C the $L_{\beta'}$ bilayer gel exhibits maximum hydration at 30 wt% water (bilayer periodicity, 64.0 Å). At 60°C, the L_α bilayer liquid crystal phase shows maximum hydration at 36 wt% water (bilayer periodicity, 60.0 Å). Thus, clearly the low temperature 'crystal' bilayer phase has a reduced maximum hydration level, corresponding to 11 water molecules/molecule DPPC. Corresponding maximum hydration values for the $L_{\beta'}$ and L_α bilayer phases are 19 and 25 molecules H_2O/molecule DPPC, respectively.

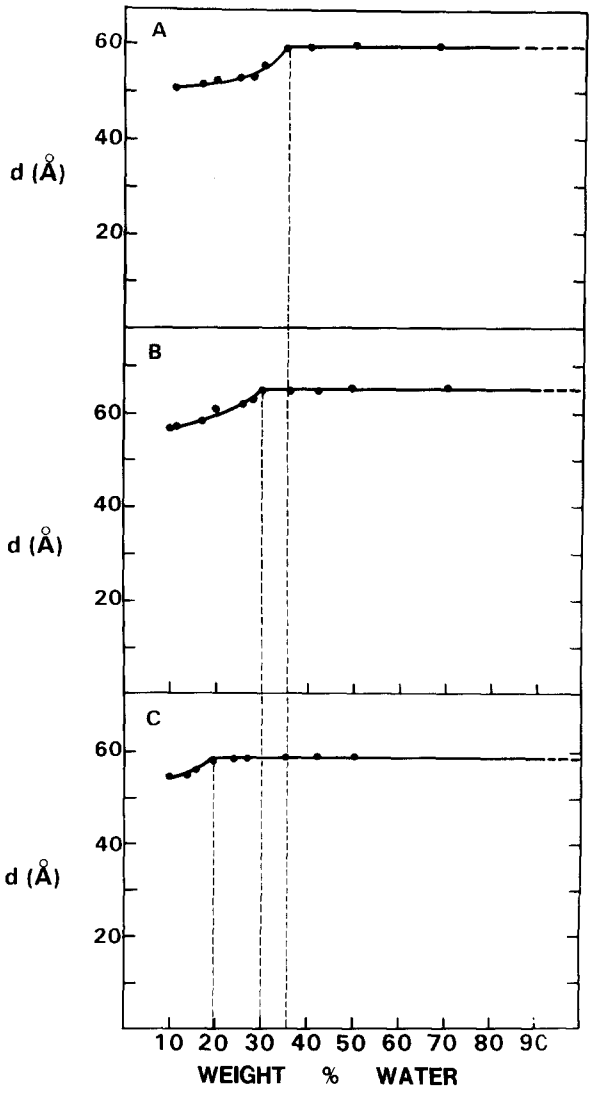

Fig. 10. Plot of bilayer periodicity, d(Å), of DPPC as a function of hydration (wt% H_2O). (A) At 60°C in the L_α liquid crystal bilayer phase; (B) at 20°C in the $L_{\beta'}$ gel bilayer phase; (C) at 4°C in the L_c 'crystal' bilayer phase. Vertical dashed lines represent the hydration limits of the L_α, $L_{\beta'}$ and L_c bilayer phases.

Discussion

The relatively slow formation of the low temperature crystalline (L_c) phase of hydrated DPPC originally described by Chen et al. [7] allows the kinetics of the $L_{\beta'} \rightarrow L_c$ conversion to be followed

using both scanning calorimetry and fast-recording X-ray diffraction methods. Our protocol was designed to (i) observe the enthalpy associated with the subtransition ($L_c \rightarrow L_{\beta'}$) as a monitor of L_c phase formation using DSC, and (ii) to follow directly the structural changes accompanying the $L_{\beta'} \rightarrow L_c$ conversion at $-2°C$ using X-ray diffraction. In addition, both Füldner [8] and we [9] have suggested that formation of the L_c phase is accompanied by a decrease in hydration. X-ray diffraction studies at 4°C of the L_c phase of DPPC at different hydrations are used to determine the maximum hydration of the L_c phase. Finally, on the basis of the changes of the wide-angle reflections as hydrated DPPC converts between $L_\alpha \rightarrow P_{\beta'} \rightarrow L_{\beta'} \rightarrow L_c$ bilayer forms on cooling, a rational scheme for the hydrocarbon chain packing arrangements in all phases is proposed.

(1) Kinetics of $L_{\beta'} \rightarrow L_c$ phase change at $-2°C$

Both the DSC (Figs. 1, 2, 5, 6) and X-ray diffraction (Figs. 3, 4, 7, 8) confirm the slow kinetic behavior of the low temperature $L_{\beta'} \rightarrow L_c$ conversion. Within experimental error, both hydration-limited (27.2 wt% H_2O) and fully hydrated (48.9 wt% H_2O) DPPC show identical kinetic behavior. The enthalpy associated with the sub-transition increases with incubation time in an approximately hyperbolic manner, reaching a limiting enthalpy of 5.6–5.8 kcal/mol DPPC. In earlier studies, lower enthalpy values in the range 2.65 to 3.7 kcal/mol DPPC were observed [7–9], and it is clear that the precise thermal history, equilibration time, equilibration temperature, etc., influence the rate of the formation of the L_c phase (see Chen et al. [7] for a detailed study). Our present studies show that both the sub-transition temperature (onset and peak maximum) and enthalpy increase with increasing incubation time at $-2°C$ and under these conditions a limiting value for the enthalpy is reached after approx. 2 days.

The corresponding structural changes show a somewhat different and perhaps more complicated pattern of behavior (see Figs. 4 and 8). For the first 1.5 to 2 h at $-2°C$, no significant change in bilayer periodicity occurs. However, marked changes in the wide-angle diffraction pattern do occur, indicating rapid modifications in the hydrocarbon chain packing mode. The 1/4.18 and 1/4.08 $Å^{-1}$ lines characteristic of the $L_{\beta'}$ phase separate significantly over this time scale, reaching values of approx. 1/4.3 and 1/4.0 $Å^{-1}$. These rapid initial changes are followed by slower alterations in the wide angle diffraction pattern, and over this second time period (2–12 h) the bilayer periodicity does show a continuous decrease from 62–63 Å (depending on the initial hydration, cf. Figs. 4 and 8) to a limiting bilayer periodicity of 59.5 Å (independent of initial hydration (cf. Figs. 4 and 8)). Thus, in this region, further modifications to the chain packing are now accompanied by a decrease in the interbilayer hydration. Only minor changes in both the bilayer periodicity and the wide angle reflections occur after 12–14 h at $-2°C$ (see Figs. 4 and 8). Therefore, over the time scale (16–64 h) in which the sub-transition enthalpy almost doubles (approx. 3 to 6 kcal/mol DPPC), no changes in the diffraction pattern characteristic of L_c phase are observed. It is probable that very small changes in molecular and hydrocarbon chain lateral packing, undetectable by X-ray diffraction, are contributing significantly to the overall stability of the 'crystalline' L_c form and the enthalpy required to convert it to the $L_{\beta'}$ form.

(2) Hydration of L_c phase of DPPC

From the DSC data presented in Figs. 1, 5 and 9, it is clear that the sub-transition is observed for DPPC at all hydration levels in the range 10.1 to 93.9 wt%. Thus, extensive amounts of water are not required for the formation of this phase. The structural parameters defining this phase may be studied as a function of hydration. The wide angle X-ray diffraction patterns of all hydrated DPPC samples at 4°C are characteristic of the L_c phase (Refs 8, 9 and Figs. 3 and 7). However, at low hydration levels the bilayer periodicity does increase with increasing hydration, reaching a limiting value of 59.3 Å at 20.0 wt% H_2O (Fig. 10). This corresponds to 11 water molecules/molecule DPPC and probably represents tightly bound water molecules at the polar lipid interface [12]. As shown clearly in Fig. 10, the L_c phase of DPPC hydrates significantly less than the $L_{\beta'}$ phase (19 mol H_2O/mol DPPC). Thus, as suspected from earlier studies [8,9], fully hydrated DPPC loses 8 mol H_2O/mol DPPC as the hydrated $L_{\beta'}$ bilayer phase slowly converts to the less hydrated stable

'crystalline' L_c phase. It is probable that the inter-bilayer region in the L_c phase is occupied exclusively by tightly bound, H-bonded water molecules providing a coupling between adjacent bilayer polar groups similar to that exhibited by crystalline DMPC dihydrate [13].

(3) Molecular and hydrocarbon chain packing

On the basis of previous X-ray diffraction [1,2,4–6,14] and other data [15] on DPPC, the molecular arrangements shown in Fig. 11 have been proposed for (i) the $L_{\beta'}$ hydrated bilayer gel phase with tilted, quasi-orthorhombic packing of the hydrocarbon chains; (ii) the $P_{\beta'}$ hydrated rippled bilayer gel phase with perhaps less tilted, hexagonal packing of the hydrocarbon chains; and (iii) the L_α hydrated liquid crystal bilayer phase with 'melted' hydrocarbon chains arranged in a quasi-hexagonal disordered lattice.

Conclusions concerning the hydrocarbon chain packing arrangement of hydrated DPPC have been derived from the rather limited X-ray diffraction data in the wide angle region and comparisons with known chain packing modes in the crystalline state (for a review of the latter, see Ref. 16). In general, it has not been possible to follow directly the progressive conversion of one chain packing mode to another. The slow kinetics of the $L_{\beta'} \rightarrow L_c$ conversion allow the X-ray diffraction changes corresponding to hydrocarbon chain packing changes to be monitored (see Figs. 4 and 8). It is convenient first to discuss the proposed packing arrangements in the L_α, $P_{\beta'}$ and $L_{\beta'}$ phases of hydrated DPPC.

L_α phase

If we treat the broad $1/4.5$ Å^{-1} reflection observed for the L_α phase of DPPC as true Bragg diffraction from a hexagonal lattice, the hexagonal cell can be transformed to a two-dimensional rectangular lattice of dimensions $a = 9.02$ Å, $b = 10.42$ Å, $\gamma = 90°$, containing 4 hydrocarbon chain projections (see Fig. 11D). This corresponds to an area of 23.5 Å^2/hydrocarbon chain.

$P_{\beta'}$ phase

In the $P_{\beta'}$ phase of hydrated DPPC only a single sharp reflection at $1/4.19$ Å^{-1} is observed. In this

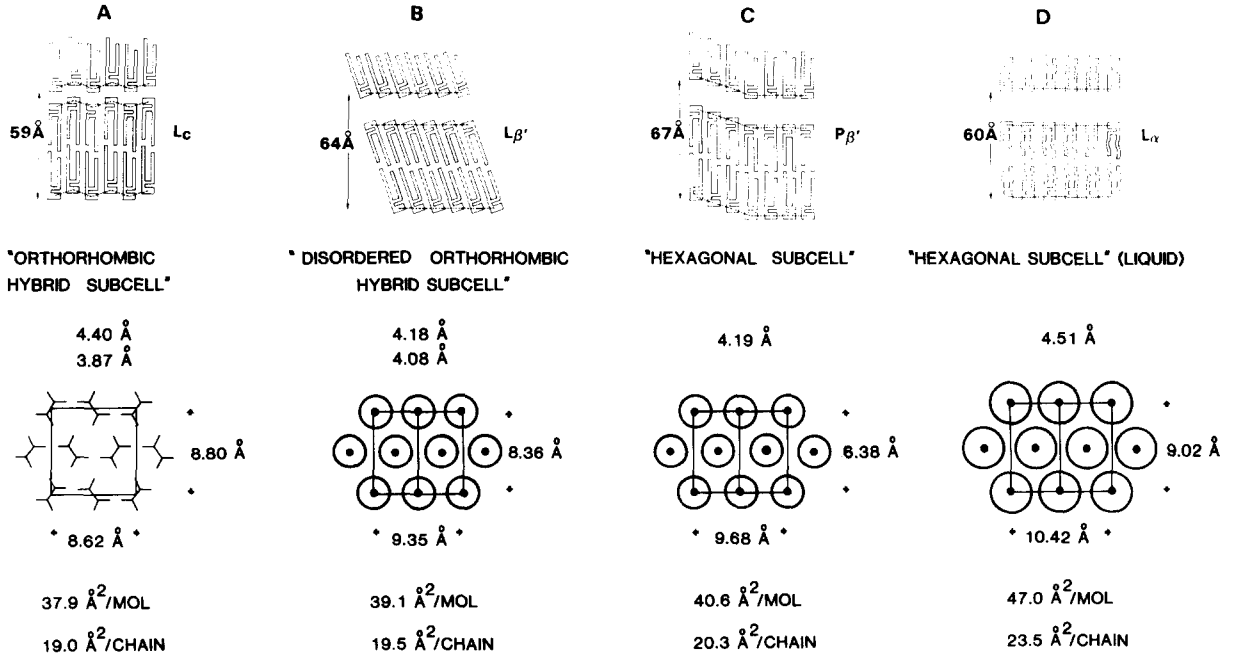

Fig. 11. Proposed molecular (top) and hydrocarbon chain (bottom) packing arrangements in L_c 'crystal', $L_{\beta'}$ gel, $P_{\beta'}$ gel and L_α liquid crystal bilayer phases. The wide angle diffraction data, derived sub-cell parameters and areas/hydrocarbon chain corresponding to the different phases are listed.

phase the hydrocarbon chains are mainly in the all-*trans* conformation, although some *gauche* conformers may be present, and packed in a regular hexagonal lattice. Again, assuming that the observed reflection at $1/4.19$ Å^{-1} is the 1,0 reflection, the hexagonal lattice can be transformed to a rectangular lattice of dimensions $a = 8.38$ Å, $b = 9.68$ Å, $\gamma = 90°$ (see Fig. 11C). As expected, the calculated area of 20.3 Å^2/chain is significantly less than that of the hydrocarbon chain area in the L_α phase. It is probable that the hydrocarbon chain lattice in the $P_{\beta'}$ phase is imperfect in that the lattice sites are occupied by chains in 'random' orientation, i.e. rotational chain disorder exists.

$L_{\beta'}$ phase

Looking into the $L_{\beta'}$ phase provides the first clear evidence of a non-hexagonal lattice. Although the strong $1/4.18$ Å^{-1} reflection characteristic of the $P_{\beta'}$ is still present, a shoulder appears at $1/4.08$ Å^{-1}. Assuming that the two reflections represent diffraction from (2,0) and (1,2) lattice planes (see Fig. 11B) a two-dimensional rectangular lattice $a = 8.36$ Å, $b = 9.35$ Å, $\gamma = 90°$ is suggested, i.e., similar to that of the hexagonal lattice of the $P_{\beta'}$ phase but with a reduced b dimension. The area per chain is reduced to 19.5 Å^2. Again, it is probable that chain orientation at each lattice site is inexact and the lateral chain packing arrangement still does not correspond to any of the precise simple and hybrid sub-cells [16,17].

L_c phase

It is clear from Figs. 4 and 8 that the $1/4.18$ Å^{-1} reflection characteristic of the $L_{\beta'}$ form changes perhaps in two stages (see above), ultimately becoming the $1/4.4$ Å^{-1} reflection characteristic of the L_c phase. Similarly we can follow the progressive conversion of the $1/4.08$ Å^{-1} reflection of the $L_{\beta'}$ phase to that at $1/3.86$ Å^{-1} characteristic of the L_c phase. At the same time other reflections appear in the wide angle region, indicative of the formation of a more ordered and probably three-dimensional lattice (see Fig. 2 in Ref. 9). Assuming the changes in these reflections represent simple alterations to the lattice parameters of the original $L_{\beta'}$ phase, we can define the hydrocarbon chain lattice in the L_c phase as $a = 8.8$ Å, $b = 8.62$ Å, $\gamma = 90°$ (Fig. 11A). There is a small reduction in the area/chain to 19.0 Å^2 compared to the chain area in the $L_{\beta'}$ phase (19.5 Å^2). In the L_c phase a precise hybrid sub-cell chain packing is likely with specific chain orientations at each lattice site, as suggested in Fig. 11A, bottom. In an earlier publication [9] we suggested that the $L_{\beta'} \rightarrow L_c$ transformation was accompanied by both formation of an ordered hydrocarbon chain lattice and dehydration, resulting in a three-dimensional crystallization of a hydrated DPPC. We expect that the molecular arrangement of this crystalline L_c form is similar, but not identical, to that of DMPC dihydrate [13] with both a decrease in molecular tilt with respect to the bilayer normal and vertical displacement of neighboring molecules (cf. Figs. 11A and 11B, top). These changes are necessary in order to accommodate the different projected areas occupied by the polar group and hydrocarbon chains [18].

Conclusion

This combined DSC and X-ray diffraction study has characterized the structural changes accompanying the slow conversion of the $L_{\beta'}$ bilayer gel phase of DPPC to a more stable low temperature crystalline L_c phase. The data illustrate clearly that the $L_{\beta'} \rightarrow L_c$ transition is accompanied by both an increase in lateral molecular order as indicated by changes in hydrocarbon chain packing and a decrease in interbilayer hydration. A combination of these two effects suggests that three-dimensional crystallization of DPPC and 11 H_2O occurs. By following the X-ray diffraction changes during the $L_{\beta'} \rightarrow L_c$ transition, the relationship between the hydrocarbon chain packing modes in these two phases is established and this in turn allows the chain packing modes in all hydrated states to be rationalized.

Finally, it is becoming clear that hydrated membrane phospholipids and sphingolipids [19–22] frequently exhibit interconversions between metastable and stable states. In most cases changes in both hydrocarbon chain packing and hydration seem to occur.

Acknowledgements

We wish to thank T. Reynolds and I. Miller for assistance in the preparation of this manuscript.

This research was supported by U.S. Public Health Service grants HL-26335, HL-07291 and HL-07429.

References

1 Chapman, D., Williams, R.M. and Ladbrooke, B.D. (1967) Chem. Phys. Lipids 1, 445–475
2 Tardieu, A., Luzzati, V. and Reman, F.C. (1973) J. Mol. Biol. 75, 711–733
3 Mabrey, S. and Sturtevant, J.M. (1976) Proc. Natl. Acad. Sci. U.S.A. 73, 3862–3866
4 Levine, Y., Bailey, A.I. and Wilkins, M.H.F. (1968) Nature 220, 577–578
5 Janiak, M.J., Small, D.M. and Shipley, G.G. (1976) Biochemistry 15, 4575–4580
6 Janiak, M.J., Small, D.M. and Shipley, G.G. (1979) J. Biol. Chem. 254, 6068–6078
7 Chen, S.C., Sturtevant, J.M. and Gaffney, B.J. (1980) Proc. Natl. Acad. Sci. U.S.A. 77, 5060–5063
8 Füldner, H.H. (1981) Biochemistry 20, 5707–5710
9 Ruocco, M.J. and Shipley, G.G. (1982) Biochim. Biophys. Acta 684, 59–66
10 Bartlett, G. (1959) J. Biol. Chem. 234, 466–469
11 Magni, R. and Sheridan, J.P. (1982) Biophys. J. 37, 11a
12 Hauser, H. (1975) in Water, A Comprehensive Treatise, Vol. 4 (Franks, F., ed.), pp. 209–303, Plenum Press, New York
13 Pearson, R.H. and Pascher, I. (1979) Nature 281, 499–501
14 Inoko, Y. and Mitsui, T. (1978) J. Phys. Soc. Jap. 44, 1918–1924
15 Luna, E. and McConnell, H.M. (1977) Biochim. Biophys. Acta 466, 381–392
16 Abrahamsson, S., Dahlen, B., Lofgren, H. and Pascher, I. (1978) Prog. Chem. Fats Other Lipids 16, 125–143
17 Hitchcock, P.B., Mason, R., Thomas, K.M. and Shipley, G.G. (1974) Proc. Natl. Acad. Sci. U.S.A. 71, 3036–3040
18 Hauser, H., Pascher, I., Pearson, R.H. and Sundell, S. (1981) Biochim. Biophys. Acta 650, 21–51
19 Harlos, K. and Eibl, H. (1980) Biochim. Biophys. Acta 601, 113–122
20 Estep, T.N., Calhoun, W.I., Barenholz, Y., Biltonen, R.L., Shipley, G.G. and Thompson, T.E. (1980) Biochemistry 19, 20–24
21 Freire, E., Bach, D., Correa-Freire, M., Miller, I. and Barenholz, Y. (1980) Biochemistry 19, 3662–3665
22 Ruocco, M.J., Atkinson, D., Small, D.M., Oldfield, E., Skarjune, R. and Shipley, G.G. (1981) Biochemistry 21, 5957–5966